MATHEMATICAL MODELING AND COMPUTING, Vol. 9, No. 3, pp. 579–593 (2022)

Dynamical analysis of an HCV model with cell-to-cell transmission and cure rate in the presence of adaptive immunity

Sadki M.[1], Harroudi S.[2], Allali K.[1]

[1]*Laboratory of Mathematics, Computer Science and Applications, FST Mohammedia, University Hassan II of Casablanca, PO Box 146, Mohammedia, Morocco*
[2]*ENCG of Casablanca, University Hassan II, Casablanca, Morocco*

(Received 10 February 2022; Accepted 15 May 2022)

In this paper, we will study mathematically and numerically the dynamics of the hepatitis C virus disease with the consideration of two fundamental modes of transmission of the infection, namely virus-to-cell and cell-to-cell. In our model, we will take into account the role of cure rate of the infected cells and the effect of the adaptive immunity. The model consists of five nonlinear differential equations, describing the interaction between the uninfected cells, the infected cells, the hepatitis C virions and the adaptive immunity. This immunity will be represented by the humoral and cellular immune responses. This work begins with proving the non-negativity and the boundedness of solutions and determining the basic reproduction number. Secondly, five equilibria are established, the local stability analysis for all the equilibria is demonstrated theoretically and numerically. Finally, we have concluded that the numerical results are coherent with our theoretical postulations.

Keywords: *cell-to-cell, cure rate, humoral immune response, cellular immune response, adaptive immunity, stability.*

2010 MSC: 34A12, 34D20, 37M05, 92-08, 92-10, 92B05 **DOI:** 10.23939/mmc2022.03.579

1. Introduction

Hepatitis C virus (HCV) is a type of virus that causes liver disease by infecting the hepatocytes. The HCV can generate both acute and chronic hepatitis. About 58 million people worldwide are infected with the chronic HCV, while 1.5 million new infections occurring each year [1]. Neumann et al. [2] affirm that liver cirrhosis can occur in 20% to 30% of people infected with chronic HCV; however, 13% of those who have liver cirrhosis can develop liver cancer. In [2], there is an earlier model for HCV viral dynamics incorporating the effect of antiviral treatment using interferon-α (IFN) and the authors confirm that the IFN blocks the production of virions more than blocking new infections. Many works dealing with viral dynamics [3–8], have taken into consideration the cure of infected cells assuming the non-cytolytic mechanism, i.e. the removal of virus without destruction of infected cell. From a biological point of view, it is assumed that infected cell can be cured or recovered and transformed back into an uninfected cell. Taking into account the cure of infected cells, [9,10] present the dynamics of HCV with a basic model that contains only three compartments, namely the uninfected cells, the infected cells and the viral load. The mode of transmission the afore-mentioned works adopted is virus-to-cell. That is why to better describe the infection, it is very important to consider another mode of transmission, that of cell-to-cell transmission [11]. In fact, there is a model which have considered both modes of transmission so as to describe the HCV dynamics with two therapies; namely interferon and ribavirin [12]. Since the adaptive immunity plays an essential role in fighting the infection, many mathematical models have included the adaptive immunity to study the viral dynamics. The adaptive immunity is represented by the humoral immune response and the cellular immune response. Firstly, the humoral immune response. As it is well known, represented by the antibodies or B cells, plays a

crucial role in reducing the amount of free viruses. Recently, Pan et al. [13] proposed a model for HCV infection, which integrates the both routes of transmission as well as the non-cytolytic cure of infected cells. Their model have taken the following form

$$\begin{cases} \dfrac{dT}{dt} = \lambda - \beta_1 TV - \beta_2 TI + \alpha I - d_1 T, \\ \dfrac{dI}{dt} = \beta_1 TV + \beta_2 TI - \alpha I - d_2 I, \\ \dfrac{dV}{dt} = kI - pVW - d_3 V, \\ \dfrac{dW}{dt} = cVW - d_4 W. \end{cases} \tag{1}$$

Here T and I represent the density of susceptible hepatocytes and infected hepatocytes, respectively. V is the viral load and W describes the antibody response. The susceptible hepatocytes are assumed to be generated at a constant rate λ and die naturally at the rate d_1. Each susceptible hepatocyte becomes infected either by one free virus at rate β_1 or by direct contact with an infected cell at rate β_2. Infected cells become cured through the non-cytolytic mechanism at rate α and they die naturally at rate d_2. Free virions are produced at rate k and they decay at rate d_3. The humoral immune response is induced by the formation of B cells at a rate c, and they are cleared at rate d_4. The virions get neutralized by the effect of B cells at a rate p. Secondly, the cellular immune response, represented by cytotoxic T-lymphocytes (CTL) or T cells, is vital in reducing the amount of infected cells. Avendano et al. [14] have formulated a model to describe the dynamics of HCV considering the effect of CTL response and to analyze the effect of the treatment IFN from a theoretical point of view. Several papers [15–19], have modeled the HCV dynamics by including both CTL and antibodies. For instance, a model proposed by Wodarz [17] have explored the role of both humoral and cellular immune responses in the dynamics of both acute and chronic HCV infection. Later, Yousfi et al. [19] have suggested a mathematical analysis of the latter model. Similarly, Meskaf et al. [15], have explored global stability analysis of the model [17]; they have included the effect of therapy. It will be more realistic to consider the effect of both humoral and cellular immune response simultaneously, and so our contribution in this paper is to study the model (1) along with the cellular immune response. Accordingly, our model for HCV dynamics incorporates both virus-to-cell and cell-to-cell transmission, the possibility of cure of infected cells, along with the effect of adaptive immunity. Our proposed model is governed by the system of ordinary differential equations

$$\begin{cases} \dfrac{dT}{dt} = \lambda - \beta_1 TV - \beta_2 TI + \alpha I - d_1 T, \\ \dfrac{dI}{dt} = \beta_1 TV + \beta_2 TI - qIZ - \alpha I - d_2 I, \\ \dfrac{dV}{dt} = kI - pVW - d_3 V, \\ \dfrac{dW}{dt} = cVW - d_4 W, \\ \dfrac{dZ}{dt} = gIZ - d_5 Z. \end{cases} \tag{2}$$

Here our new variable Z represents the cellular immune response (CTLs). The CTL cells are activated through the development of T cell at a rate g and get neutralized by the effect of T cells at a rate q. Finally, d_5 is the rate of the natural death of each T cell. The model (2) is represented graphically in Figure 1. The initial conditions are taken as $(T(0), I(0), V(0), W(0), Z(0)) \in \mathbb{R}^5$. It is worthy summarizing the works already done in this field in Table 1.

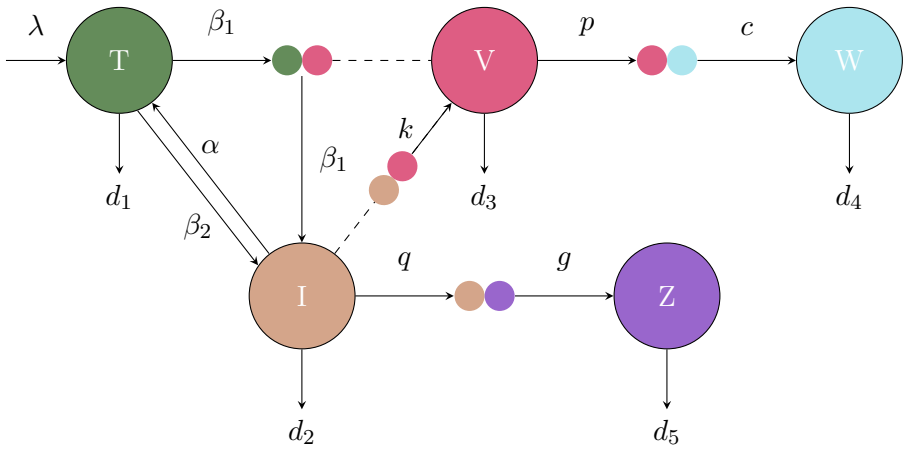

Fig. 1. Schematic representation of the studied HCV infection.

Table 1. Comparison of the various previous HCV models.

Basic model	Humoral response	Cellular response	Cell-to-cell	Cure	References
Yes	No	Yes	No	No	[23]
Yes	Yes	Yes	No	No	[4, 5, 8, 12, 13]
Yes	No	No	Yes	No	[15]
Yes	No	No	No	Yes	[16, 17]
Yes	No	No	Yes	Yes	[18]
Yes	Yes	No	Yes	Yes	[3]
Yes	Yes	Yes	Yes	Yes	Present model

The paper is organized as follows. The next section deals with the non-negativity and boundedness of solutions. In Section 3, we will present the basic reproduction number and the equilibria. Section 4 is concerned with the local stability of each equilibrium, followed by Section 5 which gives some numerical simulations. The last section is a conclusive summary of the present work.

2. Non-negativity and boundedness of solutions

Since the model (2) interprets the biological evolution of cells, only bounded positive solutions make the system of equations valid. Hence, in this section, we will prove that our system has positive and bounded solutions. First, the system (2) with non-negative initial condition has a unique local solution $(T(t), I(t), V(t), W(t), Z(t))$, because the system right-hand side is a locally Lipschitz function. The result of non-negativity and boundedness of solutions is given as follows.

Theorem 1. *If $S(0) \geqslant 0$, $I(0) \geqslant 0$, $V(0) \geqslant 0$, $W(0) \geqslant 0$ and $Z(0) \geqslant 0$ then the solution of (2) are positive and bounded for all $t > 0$. In addition, there exists an $\varepsilon > 0$ such that $\liminf_{t\to\infty} T(t) \geqslant \varepsilon$.*

Proof. To show the non-negativity and boundedness of solutions of the system (2), we will adopt the same approach as in [13, 20]. Suppose that there exists the first time $t_V > 0$ such that $V(t_V) = 0$ and $\frac{dV(t_V)}{dt} \leqslant 0$. Accordingly from the third equation of (2) we have, $\frac{dV(t_V)}{dt} = kI(t_V) \leqslant 0$.

In the same manner, we define the first time $t_I > 0$ such that $I(t_I) = 0$ and $\frac{dI(t_I)}{dt} = T(t_I)V(t_I) \leqslant 0$. Obviously, $t_I < t_V$. Now, consider that there exists a $t_T > 0$ the first time such that $T(t_T) = 0$ and $\frac{dT(t_T)}{dt} = \lambda + \alpha I(t_T) \leqslant 0$. It is easy to see that $t_T < t_I < t_V$, consequently $I(t_T) > 0$. But we note that $\frac{dT(t_T)}{dt} = \lambda + \alpha I(t_T) > 0$, which contradicts the definition of t_T itself. Thus V is a non-negative function. So, $I(t) \geqslant 0$ and then $T(t) \geqslant 0$.

From the fourth equation of the system (2),

$$W(t) = W(0) \exp\left\{ \int_0^t [cV(s) - d_4]\, ds \right\} \geqslant 0.$$

For the last equation of the system (2),

$$Z(t) = Z(0) \exp\left\{ \int_0^t [gI(s) - d_5]\, ds \right\} \geqslant 0.$$

Therefore, $T(t)$, $I(t)$, $V(t)$, $W(t)$ and $Z(t)$ are positive.

In order to demonstrate the boundedness of the solution, we can assume that there exist a function X such as, $X(t) = T(t) + I(t) + \frac{q}{g}Z$. From the equations of the system (2),

$$\frac{dX(t)}{dt} = \lambda - d_1 T(t) - d_2 I(t) - d_5 \frac{q}{g} Z \leqslant \lambda - d_X X(t), \quad \text{where} \quad d_X = \min\{d_1, d_2, d_5\}.$$

Therefore, $\limsup_{t\to\infty} X(t) \leqslant \frac{\lambda}{d_X}$.

In similar manner, it can be shown that for $Y(t) = V(t) + \frac{p}{c}W(t)$,

$$\frac{dY(t)}{dt} = kI(t) - d_3 V(t) - \frac{d_4 p}{c} Z(t) \leqslant \frac{k\lambda}{d_X} - d_Y Y(t), \quad \text{where} \quad d_Y = \min\{d_3, d_4\}.$$

Hence, $\limsup_{t\to\infty} Y(t) \leqslant \frac{\lambda k}{d_X d_Y}$.

We have established that the solution of our system (2) is bounded and positive for all $t > 0$.

Also, from the first equation of (2), we get

$$\begin{aligned} \frac{dT(t)}{dt} &\geqslant \lambda - \beta_1 T(t) V(t) - \beta_2 T(t) I(t) - d_1 T(t) \\ &\geqslant \lambda - (d_1 + \beta_1 V_u + \beta_2 I_u)\, T(t) \quad \text{for all} \quad t, \end{aligned}$$

where, $I_u = \frac{\lambda}{d_X}$ and $V_u = \frac{\lambda k}{d_X d_Y}$ are respectively the higher bounds of $I(t)$ and $V(t)$. Then we obtain, $\liminf_{t\to\infty} T(t) \geqslant \frac{\lambda}{d_1 + \beta_1 V_u + \beta_2 I_u}$, this confirms that there exists an $\varepsilon > 0$ such that $\liminf_{t\to\infty} T(t) \geqslant \varepsilon$. ■

In what follows, we will study our HCV mathematical model (2) in the following closed region

$$\mathcal{D} = \left\{ (T(t), I(t), V(t), W(t), Z(t)) \in \mathbb{R}^5_+ : 0 \leqslant T(t), I(t) \leqslant \frac{\lambda}{d_X}, 0 \leqslant V(t) \leqslant \frac{\lambda k}{d_X d_Y}, \right.$$
$$\left. 0 \leqslant W(t) \leqslant \frac{c\lambda k}{p d_X d_Y}, 0 \leqslant Z(t) \leqslant \frac{c\lambda k}{p d_X d_Y} \right\}.$$

3. The basic reproduction number and the equilibria

In this section, we present the basic reproduction number associated to our model (2) as well as its equilibria and the conditions that guarantee the existence of this equilibria.

3.1. The basic reproduction number

The proposed model (2) has one disease free equilibrium (DFE) defined by

$$E_0 = (T_0, I_0, V_0, W_0, Z_0) = \left(\frac{\lambda}{d_1}, 0, 0, 0, 0 \right).$$

We will look now for the basic reproduction number which measures the average number of new HCV infected cells generated by a unique typical infected cell in a completely susceptible cells environment. This parameter is symbolized by $\mathcal{R}_0$. To calculate it, we will apply the next generation matrix

approach [27, 29]. However, the associated equations with infection are

$$\frac{dI}{dt} = \beta_1 TV + \beta_2 TI - d_2 I - qIZ - \alpha I = \mathcal{F}_1 - \mathcal{V}_1,$$
$$\frac{dV}{dt} = kI - d_3 V - pVZ = \mathcal{F}_2 - \mathcal{V}_2,$$

where $\mathcal{F}_1 = \beta_1 TV + \beta_2 TI$, $\mathcal{V}_1 = qIZ + d_2 I + \alpha I$, $\mathcal{F}_2 = 0$, $\mathcal{V}_2 = d_3 V + pVZ - kI$.

Knowing that $\mathcal{R}_0 = \rho(FV^{-1})$, where $\rho(A)$ is the spectral radius of matrix A. In our situation we have

$$F = \begin{pmatrix} \frac{\partial \mathcal{F}_1}{\partial I}\Big|_{E_0} & \frac{\partial \mathcal{F}_1}{\partial V}\Big|_{E_0} \\ \frac{\partial \mathcal{F}_2}{\partial I}\Big|_{E_0} & \frac{\partial \mathcal{F}_2}{\partial V}\Big|_{E_0} \end{pmatrix} = \begin{pmatrix} \frac{\lambda\beta_2}{d_1} & \frac{\lambda\beta_1}{d_1} \\ 0 & 0 \end{pmatrix},$$

$$V = \begin{pmatrix} \frac{\partial \mathcal{V}_1}{\partial I}\Big|_{E_0} & \frac{\partial \mathcal{V}_1}{\partial V}\Big|_{E_0} \\ \frac{\partial \mathcal{V}_2}{\partial I}\Big|_{E_0} & \frac{\partial \mathcal{V}_2}{\partial V}\Big|_{E_0} \end{pmatrix} = \begin{pmatrix} d_2 + \alpha & 0 \\ -k & d_3 \end{pmatrix}.$$

Therefore

$$\mathcal{R}_0 = \frac{\lambda\,(\beta_1 k + \beta_2 d_3)}{d_1 d_3\,(d_2 + \alpha)} = \frac{k\beta_1 T_0}{d_3\,(d_2 + \alpha)} + \frac{\beta_2 T_0}{d_2 + \alpha} = \mathcal{R}_{01} + \mathcal{R}_{02}.$$

The basic reproduction number is the sum of two quantities $\mathcal{R}_{01}$ and $\mathcal{R}_{02}$, the first one is related to virus-to-cell infection; while the second one is concerned with cell-to-cell transmission. Biologically, $\mathcal{R}_{01}$ measures the average number of secondary infected cells caused by a free virus in a completely susceptible cells environment. The second number $\mathcal{R}_{02}$ represents the average number of secondary infected cells generated by one infected cell in a completely susceptible cells environment.

In the sequel of the paper, we will define some thresholds parameters. The humoral immune reproduction number represented by $R^W = \frac{ck\lambda(\beta_1 k+\beta_2 d_3)}{ckd_1 d_3(d_2+\alpha)+d_2 d_3 d_4(\beta_1 k+\beta_2 d_3)}$, which represents the average of secondary generated infected cells in the presence of the humoral immune response. The cellular immune reproduction number is defined by $R^{CTL} = \frac{g\lambda(\beta_1 k+\beta_2 d_3)}{gd_1 d_3(d_2+\alpha)+d_2 d_5(\beta_1 k+\beta_2 d_3)}$, which represents the average number of secondary generated infected cells in the presence of the cellular immune response. Also, we define the threshold $R_1^{CTL,W} = \frac{qI_2}{d_5}$, as the average number of secondary generated infected cells in the presence of both humoral and cellular immune responses in the case of CTL response is more dominant [17]. Finally, the threshold $R_2^{CTL,W} = \frac{ckd_5}{gd_3 d_4}$, represents the average number of secondary generated infected cells in the presence of both humoral and cellular immune responses with the antibodies response is significantly more dominant.

3.2. The free equilibrium and the endemic equilibria

The model (2) admits five equilibrium points, namely

1. The disease-free equilibrium, $E_0 = (T_0, I_0, V_0, W_0, Z_0)$, where $T_0 = \frac{\lambda}{d_1}$, $I_0 = V_0 = W_0 = Z_0 = 0$.
2. The immune response free equilibrium, $E_1 = (T_1, I_1, V_1, W_1, Z_1)$, where $T_1 = \frac{d_3(d_2+\alpha)}{\beta_1 k+\beta_2 d_3}$, $I_1 = \frac{d_1 T_1}{d_2}\left[\frac{\lambda(\beta_1 k+\beta_2 d_3)}{d_1 d_3(d_2+\alpha)} - 1\right]$, $V_1 = \frac{k}{d_3} I_1$, $W_1 = 0$ and $Z_1 = 0$. This endemic equilibrium exists if $\mathcal{R}_0 \geqslant 1$.
3. The infected equilibrium with humoral immune response, $E_2 = (T_2, I_2, V_2, W_2, Z_2)$, where $T_2 = \frac{(d_2+\alpha)I_2}{\beta_1 V_2+\beta_2 I_2}$, $I_2 = \frac{-m_2+\sqrt{m_2^2+4m_1 m_3}}{2m_1}$, $V_2 = \frac{d_4}{c}$, $W_2 = \frac{d_3}{p}\left(\frac{ck}{d_3 d_4} I_2 - 1\right)$ and $Z_2 = 0$, with $m_1 = \beta_2 c d_2$, $m_2 = \beta_1 d_2 d_4 + cd_1\,(d_2 + \alpha) - \lambda\beta_2 c$, $m_3 = \lambda\beta_1 d_4$.
   Here, $R_1 = \frac{ck}{d_3 d_4} I_2$ represents the viral reproduction number in the chronic stage of infection with the effect of humoral immune response. Obviously, E_2 exists if $R_1 \geqslant 1$.
4. The infected equilibrium with cellular immune response $E_3 = (T_3, I_3, V_3, W_3, Z_3)$, where $T_3 = \frac{\lambda+\alpha I_3}{\beta_1 V_3+\beta_2 I_3+d_1}$, $I_3 = \frac{d_5}{g}$, $V_3 = \frac{k}{d_3} I_3$, $W_3 = 0$ and $Z_3 = \left(\frac{d_2+\alpha}{q}\right)\left(\frac{(\beta_1 V_3+\beta_2 I_3)T_3}{(d_2+\alpha)I_3} - 1\right)$. Here, $R_2 =$

$\frac{(\beta_1 V_3+\beta_2 I_3)T_3}{(d_2+\alpha)I_3}$ represents the viral reproduction number in the chronic stage of infection with the effect of cellular immune response to infected cells. In fact, E_3 exists if $\mathcal{R}_2 \geqslant 1$.

5. The infected equilibrium with both humoral and cellular immune response $E_4 = (T_4, I_4, V_4, W_4, Z_4)$, where $T_4 = \frac{\lambda+\alpha I_4}{\beta_1 V_4+\beta_2 I_4+d_1}$, $I_4 = \frac{d_5}{g}$, $V_4 = \frac{d_4}{c}$, $W_4 = \frac{d_3}{p}\left(\frac{kI_4}{d_3 V_4}-1\right)$, and $Z_4 = \left(\frac{d_2+\alpha}{q}\right)\times \left(\frac{(\beta_1 V_4+\beta_2 I_4)T_4}{(d_2+\alpha)I_4}-1\right)$. Here, $R_3 = \frac{(\beta_1 V_4+\beta_2 I_4)T_4}{(d_2+\alpha)I_4}$ represents the viral reproduction number in the chronic stage of infection with the effect of both humoral and cellular immune response and infected cells. If $\mathcal{R}_3 \geqslant 1$ and $R_2^{CTL,W} \geqslant 1$ then E_4 exists.

4. Local stability analysis

In this section, we will study the local stability analysis of the equilibria by applying Routh–Hurwitz Theorem [24]. First, we linearize the system (2), we have the following Jacobian matrix

$$\begin{bmatrix} -\beta_1 V-\beta_2 I-d_1 & -\beta_2 T+\alpha & -\beta_1 T & 0 & 0 \\ \beta_1 V+\beta_2 I & \beta_2 T-qZ-d_2-\alpha & \beta_1 T & 0 & -qI \\ 0 & k & -d_3-pW & -pV & 0 \\ 0 & 0 & cW & cV-d_4 & 0 \\ 0 & gZ & 0 & 0 & gI-d_5 \end{bmatrix}.$$

Additionally, we will need to the arithmetic and geometric means inequality, which states that the geometric mean of n positive real numbers $x_1, x_2, \ldots, x_n$ is less than their arithmetic mean

$$\frac{1}{n}\left(\sum_{i=1}^{n} x_i\right) \geqslant \left(\prod_{i=1}^{n} x_i\right)^{\frac{1}{n}}.$$

This inequality becomes equality if all the real numbers $x_1, x_2, \ldots, x_n$ are equals. Besides, we can see that if $\prod_{i=1}^{n} x_i = 1$, then the inequality becomes $\sum_{i=1}^{n} x_i \geqslant n$.

Theorem 2. *The disease-free equilibrium E_0 is locally asymptotically stable when $R_0 < 1$ and unstable when $R_0 > 1$.*

Proof. The characteristic equation at E_0 is identified by

$$(x+d_1)(x+d_4)(x+d_5)\left(x^2+A_1 x+A_2\right)=0,$$

where

$$\begin{aligned} A_1 &= d_2+d_3+\alpha-\frac{\lambda\beta_2}{d_1} \\ &= d_3+(d_2+\alpha)(1-\mathcal{R}_0+R_{01}), \\ A_2 &= d_3(d_2+\alpha)-\frac{\lambda}{d_1}(\beta_1 k+\beta_2 d_3) \\ &= d_3(d_2+\alpha)(1-\mathcal{R}_0). \end{aligned}$$

The characteristic equation, has five eigenvalues, three of them are obviously negative $x_1 = -d_1$, $x_2 = -d_4$, and $x_3 = -d_5$. Observing that if $\mathcal{R}_0 < 1$, then $A_1 > 0$ and also $A_2 > 0$. Hence, the remaining other eigenvalues will have negative real parts. In conclusion, the DFE E_0 is locally asymptotically stable when $\mathcal{R}_0 < 1$ and unstable when $\mathcal{R}_0 > 1$. ∎

Theorem 3. *The immune response free equilibrium E_1 is locally asymptotically stable when $R_0 > 1$, $R^W < 1$ and $R^{CTL} < 1$ and unstable when $R^{CTL} > 1$ or $R^W > 1$.*

Proof. The characteristic equation at E_1 is identified by

$$(x+d_4-cV_1)(x+d_5-gI_1)\left(x^3+B_1x^2+B_2x+B_3\right)=0,$$

where

$$\begin{aligned}
B_1 &= d_1 + d_2 + d_3 + \alpha + \beta_1 V_1 + \beta_2 I_1 - \beta_2 T_1 \\
&= d_1 + d_3 + (d_2 + \alpha)\frac{R_{01}}{R_0} + \frac{d_1}{d_2}(d_2 + \alpha)(R_0 - 1), \\
B_2 &= (d_2 + d_3)(\beta_1 V_1 + \beta_2 I_1) + d_1(d_2 + d_3 + \alpha - \beta_2 T_1) \\
&= d_1 d_3 + d_1(d_2 + \alpha)\frac{R_{01}}{R_0} + \frac{d_1}{d_2}(d_2 + d_3)(d_2 + \alpha)(R_0 - 1), \\
B_3 &= d_2 d_3(\beta_1 V_1 + \beta_2 I_1) \\
&= d_1 d_3(d_2 + \alpha)(R_0 - 1).
\end{aligned}$$

Two first eigenvalues are $cV_1 - d_4$ and $gI_1 - d_5$, which can be rewritten as

$$\begin{aligned}
cV_1 - d_4 &= \frac{\lambda ck}{d_2 d_3 R^W}\left(R^W - 1\right) && \text{negative when} \quad R^W < 1, \\
gI_1 - d_5 &= \frac{g\lambda}{d_2 R^{CTL}}\left(R^{CTL} - 1\right) && \text{negative when} \quad R^{CTL} < 1.
\end{aligned}$$

The other eigenvalues are the roots of the cubic equation $x^3 + B_1 x^2 + B_2 x + B_3 = 0$.

Clearly $B_1, B_3 > 0$ if $R_0 > 1$. Furthermore

$$\begin{aligned}
B_1 B_2 - B_3 = {} & d_1 d_3(d_1 + d_3) + d_1(d_1 + d_3)(d_2 + \alpha)\frac{R_{01}}{R_0} + \frac{d_1^2}{d_2^2}(d_2 + d_3)(d_2 + \alpha)^2(R_0 - 1)^2 \\
& + \frac{d_1^2}{d_2}(d_2 + \alpha)^2\frac{R_{01}}{R_0}(R_0 - 1) + \frac{d_1}{d_2}\left(d_1 d_2 + 2d_1 d_3 + d_3^2\right)(d_2 + \alpha)(R_0 - 1) \\
& + \frac{d_1}{d_2}\left(d_2 d_3 + d_2(d_2 + \alpha)\frac{R_{01}}{R_0}\right)\frac{R_{01}}{R_0}(d_2 + \alpha) \\
& + \frac{d_1}{d_2}\left(d_2 d_3 + d_2^2 + \alpha(d_2 + d_3)\right)\frac{R_{01}}{R_0}(d_2 + \alpha)(R_0 - 1).
\end{aligned}$$

Therefore, whenever $R_0 > 1$ we have $B_1 B_2 - B_3 > 0$ then the Routh–Hurwitz criterion implies that three roots of the cubic equation are negative when $R_0 > 1$. Additionally, if $R^W > 1$ or $R^{CTL} > 1$, then E_1 has at least one positive eigenvalue. So, we can state that the immune response free equilibrium E_1 is locally asymptotically stable when $R_0 > 1$, $R^W < 1$ and $R^{CTL} < 1$ and unstable if $R^W > 1$ or $R^{CTL} > 1$. ∎

Theorem 4. *The infected equilibrium with humoral immune response E_2 is locally asymptotically stable when $R_1 > 1$ and $R_1^{CTL,W} < 1$ and unstable when $R_1^{CTL,W} > 1$.*

Proof. The characteristic equation at E_2 is determined by

$$(x + d_5 - gI_2)\left(x^4 + C_1 x^3 + C_2 x^2 + C_3 x + C_4\right) = 0.$$

Where

$$\begin{aligned}
C_1 &= d_1 + \beta_1 V_2 + \beta_2 I_2 + \frac{kI_2}{V_2} + \frac{\beta_2 T_2 V_2}{I_2}, \\
C_2 &= (d_1 + \beta_1 V_2 + \beta_2 I_2)\frac{kI_2}{V_2} + d_2(\beta_1 V_2 + \beta_2 I_2) + cpV_2 Z_2 + \frac{d_1 \beta_1 T_2 V_2}{I_2}, \\
C_3 &= (d_1 + \beta_1 V_2 + \beta_2 I_2)cpV_2 Z_2 + d_2(\beta_1 V_2 + \beta_2 I_2)\frac{kI_2}{V_2} + \left(\frac{\beta_1 T_2 V_2}{I_2}\right)cpV_2 Z_2, \\
C_4 &= d_2(\beta_1 V_2 + \beta_2 I_2)cpV_2 Z_2 + d_1\left(\frac{\beta_1 T_2 V_2}{I_2}\right)cpV_2 Z_2.
\end{aligned}$$

The first observed eigenvalue is $gI_2 - d_5 = d_5(R_1^{CTL,W} - 1)$, which is negative when $R_1^{CTL,W} < 1$. Also, $C_1, C_4 > 0$ whenever T_2, I_2, V_2, W_2 and Z_2 are all positive when $R_1 > 1$. We have,

$$C_1C_2 - C_3 = (d_1 + \beta_1V_2 + \beta_2I_2)\left[(d_1 + \beta_1V_2 + \beta_2I_2)\frac{kI_2}{V_2} + \beta_1kT_2 + \left(\frac{kI_2}{V_2}\right)^2\right]$$
$$+ d_2(\beta_1V_2 + \beta_2I_2)\left[d_1 + \beta_1V_2 + \beta_2I_2 + \frac{\beta_1T_2V_2}{I_2}\right]$$
$$+ \frac{\beta_1T_2V_2}{I_2}\left[d_1(d_1 + \beta_1V_2 + \beta_2I_2) + d_1\left(\frac{kI_2}{V_2}\right) + d_1\left(\frac{\beta_1T_2V_2}{I_2}\right)\right] + ckpI_2Z_2.$$

Hence, $C_1C_2 - C_3 > 0$ when $R_1 > 1$.

$$(C_1C_2 - C_3)C_3 - C_1^2C_4 = ckpI_2Z_2(d_1 + \beta_1V_2 + \beta_2I_2)^2\left[d_1 + \frac{\beta_1V_2T_2}{I_2} + \frac{kI_2}{V_2}\right]$$
$$+ \frac{kI_2}{V_2}(d_1 + \beta_1V_2 + \beta_2I_2)^2(\beta_1V_2 + \beta_2I_2)\left[\frac{d_2kI_2}{V_2} + cpV_2Z_2\right]$$
$$+ \beta_1kT_2(d_1 + \beta_1V_2 + \beta_2I_2)(\beta_1V_2 + \beta_2I_2)(d_1d_2 + cpV_2Z_2)$$
$$+ \frac{d_2kI_2}{V_2}(d_1 + \beta_1V_2 + \beta_2I_2)(\beta_1V_2 + \beta_2I_2)\left[\beta_1kT_2 + \left(\frac{kI_2}{V_2}\right)^2\right]$$
$$+ \frac{\beta_1T_2V_2}{I_2}(\beta_1V_2 + \beta_2I_2)(d_1d_2 + cpV_2Z_2)\left[\beta_1kT_2 + \left(\frac{kI_2}{V_2}\right)^2\right]$$
$$+ \beta_1d_2\,\mathrm{ck}\,p(\beta_1V_2 + \beta_2I_2)T_2V_2Z_2\left[\frac{d_2(\beta_1V_2 + \beta_2I_2)}{cpV_2Z_2} + \frac{cpV_2Z_2}{d_2(\beta_1V_2 + \beta_2I_2)} - 2\right]$$
$$+ d_2ckp(d_1 + \beta_1V_2 + \beta_2I_2)(\beta_1V_2 + \beta_2I_2)I_2Z_2\left[\frac{d_2(\beta_1V_2 + \beta_2I_2)}{cpV_2Z_2} + \frac{cpV_2Z_2}{d_2(\beta_1V_2 + \beta_2I_2)} - 2\right].$$

As a result of the arithmetic and geometric means inequality, it follows that

$$\frac{d_2(\beta_1V_2 + \beta_2I_2)}{cpV_2Z_2} + \frac{cpV_2Z_2}{d_2(\beta_1V_2 + \beta_2I_2)} - 2 \geqslant 0.$$

Now, we can state that $(C_1C_2 - C_3)C_3 - C_1^2C_4 > 0$ whenever T_2, I_2, V_2, W_2 and Z_2 are positive when $R_1 > 1$. By the Routh–Hurwitz criteria E_2 is locally asymptotically stable when $R_1 > 1$ and $R_1^{CTL,W} < 1$ and unstable when $R_1^{CTL,W} > 1$. ■

Theorem 5. *The infected equilibrium with cellular immune response E_3 is locally asymptotically stable when $R_2 > 1$ and $R_2^{CTL,W} < 1$ and unstable when $R_2^{CTL,W} > 1$.*

Proof. The characteristic equation at E_3 is given by

$$(x + d_4 - cV_3)(x^4 + D_1x^3 + D_2x^2 + D_3x + D_4) = 0.$$

Where

$$D_1 = d_1 + d_3 + \beta_2I_3 + \beta_1V_3 + \frac{\beta_1V_3T_3}{I_3},$$
$$D_2 = d_1d_2 + d_1d_3 + d_2d_3 + d_1\alpha + d_3\alpha + d_1qZ_3 + qd_3Z_3 + qd_5Z_3 - d_1\beta_2T_3 - d_3\beta_2T_3 + d_2\beta_1V_3$$
$$+ d_3\beta_1V_3 - k\beta_1T_3 + q\beta_1V_3Z_3 + d_2\beta_2I_3 + d_3\beta_2I_3 + q\beta_2I_3Z_3,$$
$$D_3 = d_1d_2d_3 + d_1d_3\alpha - d_1d_3\beta_2T_3 + d_2d_3\beta_1V_3 - d_1k\beta_1T_3 + d_1d_3qZ_3 + d_1d_5qZ_3 + d_3d_5qZ_3 + d_2d_3\beta_2I_3$$
$$+ d_5q\beta_2I_3Z_3 + d_3q\beta_1V_3Z_3 + d_5q\beta_1V_3Z_3 + d_3q\beta_2I_3Z_3,$$
$$D_4 = qd_1d_3d_5Z_3 + d_3d_5\beta_2qZ_3I_3 + q\beta_1d_3d_5Z_3V_3.$$

One of the eigenvalues is, $cV_3 - d_4 = d_4(R_2^{CTL,W} - 1)$, which is negative when $R_2^{CTL,W} < 1$. Also, D_1, D_4 are positive whenever T_2, I_2, V_2, W_2 and Z_2 are all positive, that is, when $R_2 > 1$. Obviously, if $R_2^{CTL,W} > 1$ then there exists one positive eigenvalue. Thus, according to the Routh–Hurwitz Theorem, the immune response free equilibrium E_3 is locally asymptotically stable when $R_2 > 1$ and $R_2^{CTL,W} < 1$ and unstable when $R_2^{CTL,W} > 1$. ■

Theorem 6. *The infected equilibrium with both humoral and cellular immune response E_4 is locally asymptotically stable when $R_3 > 1$ and $R_2^{CTL,W} > 1$.*

Proof. The characteristic equation at E_4 is

$$x^5 + F_1x^4 + F_2x^3 + F_3x^2 + F_4x + F_5 = 0.$$

Where

$$\begin{aligned}
F_1 &= d_1 + d_3 + pW_4 + \beta_1\frac{V_4}{I_4}T_4 + \beta_2 I_4 + \beta_1 V_4,\\
F_2 &= d_1d_2 + d_1d_3 + d_2d_3 + d_1\alpha + d_3\alpha + d_1pW_4 + \alpha pW_4 + d_2pW_4 + d_4pW_4 + d_1qZ_4 + d_3qZ_4 + d_5qZ_4\\
&\quad - d_1\beta_2T_4 - d_3\beta_2T_4 - k\beta_1T_4 - p\beta_2W_4T_4 + d_2\beta_1V_4 + d_3\beta_1V_4 + d_2\beta_2I_4 + d_3\beta_2I_4 + pqW_4Z_4\\
&\quad + q\beta_1Z_4V_4 + \beta_2pI_4W_4 + q\beta_2Z_4I_4 + p\beta_1V_4W_4,\\
F_3 &= d_1d_2d_3 + d_1d_3\alpha - d_1d_3\beta_2T_4 - d_1k\beta_1T_4 + d_1\alpha pW_4 + d_4\alpha pW_4 + d_1d_2pW_4 + d_1d_4pW_4 + d_2d_4pW_4\\
&\quad + d_1d_3qZ_4 + d_1d_5qZ_4 + d_3d_5qZ_4 + d_2d_3\beta_2I_4 + d_2d_3\beta_1V_4 + d_1pqZ_4W_4 + d_4pqZ_4W_4 + d_5pqZ_4W_4\\
&\quad + d_4p\beta_1V_4W_4 + d_2d_4p\beta_1V_4W_4 + d_5q\beta_2I_4Z_4 + d_3q\beta_2I_4Z_4 - d_1p\beta_2T_4W_4 - d_4p\beta_2T_4W_4 + d_3q\beta_1V_4Z_4\\
&\quad + d_5q\beta_1V_4Z_4 + d_2p\beta_2I_4W_4 + d_4p\beta_2I_4W_4 \ + pq\beta_1V_4W_4Z_4 + pq\beta_2I_4W_4Z_4,\\
F_4 &= d_1d_2d_4pW_4 + d_1d_4p\alpha W_4 + d_1d_3d_5qZ_4 + d_1d_4pqW_4Z_4 + d_1d_5pqW_4Z_4 + d_4d_5pqW_4Z_4\\
&\quad + d_2d_4p\beta_1V_4W_4 + d_3d_5q\beta_2I_4Z_4 - d_1d_4p\beta_2T_4W_4 + d_2d_4p\beta_2I_4W_4 + d_3d_5q\beta_1V_4Z_4 + d_4pq\beta_1V_4W_4Z_4\\
&\quad + d_5pq\beta_1V_4W_4Z_4 + d_5pq\beta_2I_4W_4Z_4 + d_4pq\beta_2I_4W_4Z_4,\\
F_5 &= pqd_4d_5\beta_1V_4W_4Z_4 + pqd_5\beta_2I_4W_4Z_4 + pqd_1d_4d_5W_4Z_4.
\end{aligned}$$

It is evident that F_1 and F_5 are positive whenever T_4, I_4, V_4, W_4 and Z_4 are all positive, that is true when $R_3 > 1$ and $R_2^{CTL,W} > 1$. By the Routh–Hurwitz theorem, we have that the immune response free equilibrium E_4 is locally asymptotically stable when $R_3 > 1$ and $R_2^{CTL,W} > 1$. ∎

5. Numerical simulations

In order to clarify numerically the stability of each equilibrium to the model (2), we will present in this section several numerical results using Matlab software. In five figures below ($\boldsymbol{a}$) represents the uninfected cells, ($\boldsymbol{b}$) the infected cells, ($\boldsymbol{c}$) virions, ($\boldsymbol{d}$) B cells and finally ($\boldsymbol{e}$) T cells. The parameters of our numerical tests are shown in Table 3 and their units in Table 2 and also the taken initial condition is as follows $(T(0), I(0), V(0), W(0), Z(0)) = (30, 10, 2, 500, 400)$.

Table 2. The list of parameter units for the different numerical simulations.

Parameters	Descriptions	Units
λ	Source rate of uninfected cell	cells ml^{-1} day^{-1}
β_1	Virus-to-cell infection rate	ml virion $^{-1}$ day^{-1}
β_2	Cell-to-cell infection rate	ml cell $^{-1}$ day^{-1}
d_1	Death rate of uninfected cell	day^{-1}
d_2	Death rate of infected cell	day^{-1}
d_3	Death rate of virus	day^{-1}
d_4	Death rate of B cell	day^{-1}
d_5	Death rate of T cell	day^{-1}
q	Neutralization rate of infected cell by T cell	day^{-1}
α	Cure rate of infected cell	day^{-1}
k	Production rate of virus	virions cell^{-1} day^{-1}
p	Neutralization rate of virus by B cell	ml cell^{-1} day^{-1}
c	Development rate of B cell	ml virion^{-1} day^{-1}
g	Development rate of B cell	ml virion^{-1} day^{-1}

Table 3. The list of parameter values for the different numerical simulations.

Parameter	Fig. 2	Fig. 3	Fig. 4	Fig. 5	Fig. 6	Sources
λ	1	1	1	10	10	[17, 18]
β_1	0.01	0.01	0.01	0.01	0.01	[17, 18]
β_2	0.001	0.01	0.01	0.01	0.01	[13]
d_1	0.01	0.01	0.01	0.01	0.01	[22]
d_2	1	1	1	1	1	[22]
d_3	6	6	1	1	1	[17, 18, 22]
d_4	0.3	0.3	0.1	0.3	0.1	[17, 18, 28]
d_5	0.05	0.05	0.05	0.05	0.1	[17, 18, 28]
q	$5.4 \cdot 10^{-4}$	$5.4 \cdot 10^{-4}$	$5.4 \cdot 10^{-4}$	$5.4 \cdot 10^{-4}$	$5.4 \cdot 10^{-4}$	[16]
α	0.01	0.01	0.01	0.01	0.01	[23]
k	2.9	2.9	2.9	2.9	2.9	[22]
p	0.006	0.006	0.006	0.006	0.006	[28]
c	0.1	0.1	0.1	0.01	0.01	[28]
g	0.015	0.015	0.015	0.015	0.015	[28]

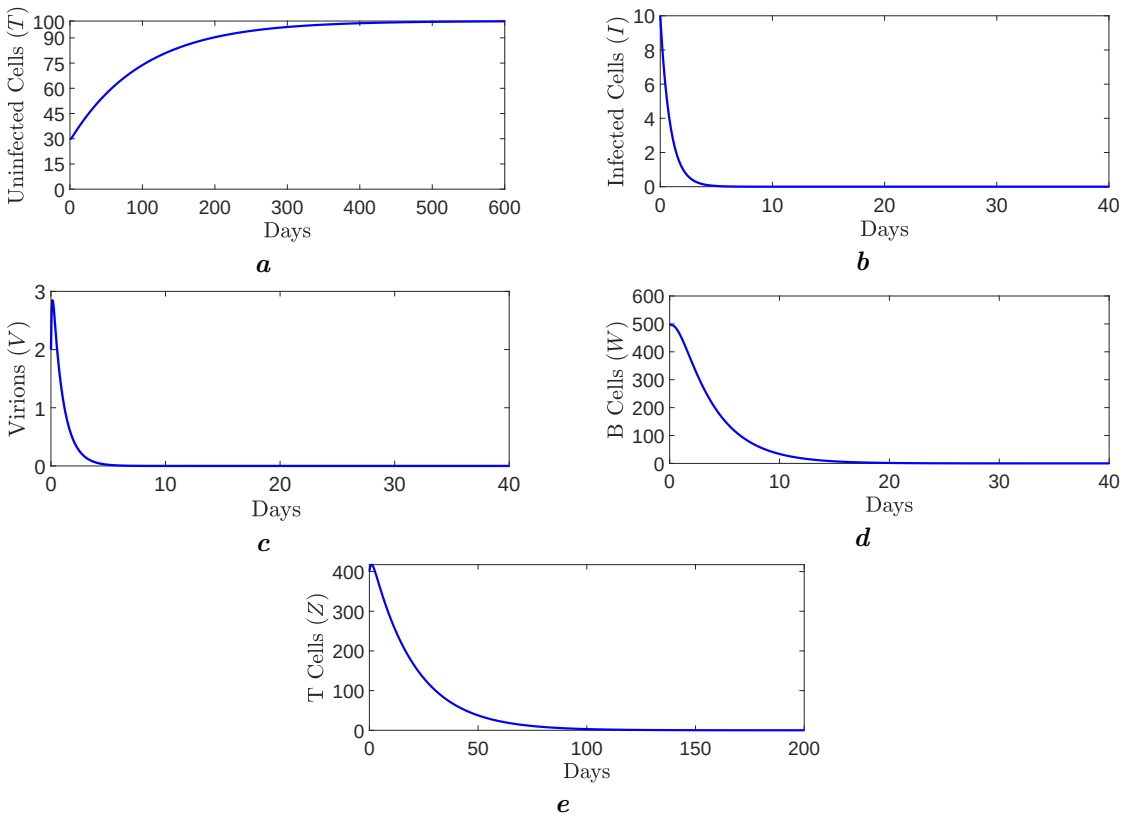

Fig. 2. The infection dynamics illustrating the stability of DFE equilibrium E_0.

In order to illustrate the stability of DFE equilibrium E_0, we will use the parameter values from Table 3 which leads to $\mathcal{R}_0 = 0.5776$. Hence, the basic reproduction number is less than unity which predicts theoretically the stability of the DFE equilibrium E_0. We clearly see from Figure 2 that the number of the uninfected cells increases progressively to reach their maximal level $\frac{\lambda}{d_1} = 100$. Besides, the concentration level of the infected cells, free virions, B cells and T cells is decreased towards zero. This simulation concludes that the solutions of the system (2) converge to the disease-free equilibrium $E_0 = (100, 0, 0, 0, 0)$. Therefore, our first numerical simulations support the theoretical result already mentioned in Theorem 2.

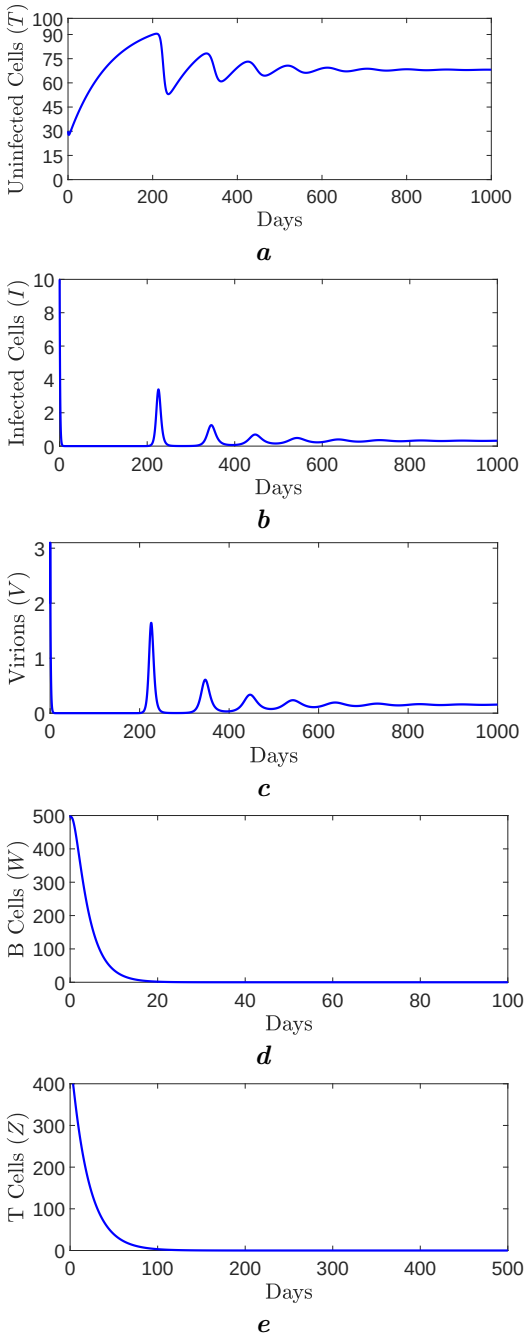

Fig. 3. The infection dynamics illustrating the stability of the first endemic equilibrium E_1.

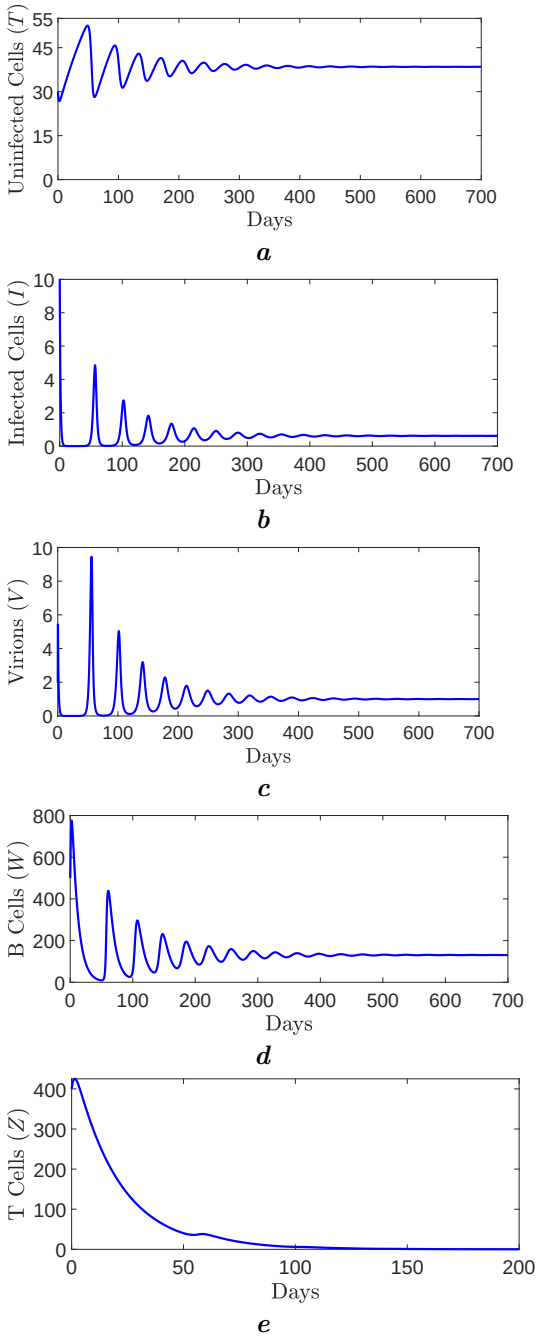

Fig. 4. The infection dynamics illustrating the stability of the second endemic equilibrium E_2.

Within the parameters indicated in Table 3, we can calculate the following thresholds $\mathcal{R}_0 = 1.4686$, $\mathcal{R}^W = 0.1608$ and $\mathcal{R}^{CTL} = 0.2491$, which means $\mathcal{R}_0 > 1$, $\mathcal{R}^W < 1$ and $\mathcal{R}^{CTL} < 1$, this predicts the theoretical stability of the first disease equilibrium E_1. We can remark from Figure 3 that the uninfected, infected cells and virions show a damped oscillatory behavior and converge to their respective coordinates of the equilibrium point $E_1 = (68.1599, 0.3220, 0.1556, 0, 0)$. We also observe that the concentrations of B cells and T cells converge towards zero. Consequently, the simulation is in good agreement with the theoretical result already stated in Theorem 3.

The following thresholds can be calculated using the parameters listed in Table 3, $\mathcal{R}_1 = 1.7843$ and also $\mathcal{R}_1^{CTL,W} = 0.1846$. Which means that $\mathcal{R}_1 > 1$ and $\mathcal{R}_1^{CTL,W} < 1$, this reflects the stability of E_2 as already pointed out in Theorem 4. Indeed, Figure 4 shows the behavior of the infection corresponding to the stability of the disease equilibrium E_2, we notice that after some periods of oscillations, the

functions that describe uninfected cells, infected cells, virions, antibodies and CTL cells are approaching respectively to their own coordinates of the infected steady state $E_2 = (38.4721, 0.6153, 1, 130.7182, 0)$. Also, we can see easily that when the quantities of virions increase, the antibody response is activated in order to neutralize them.

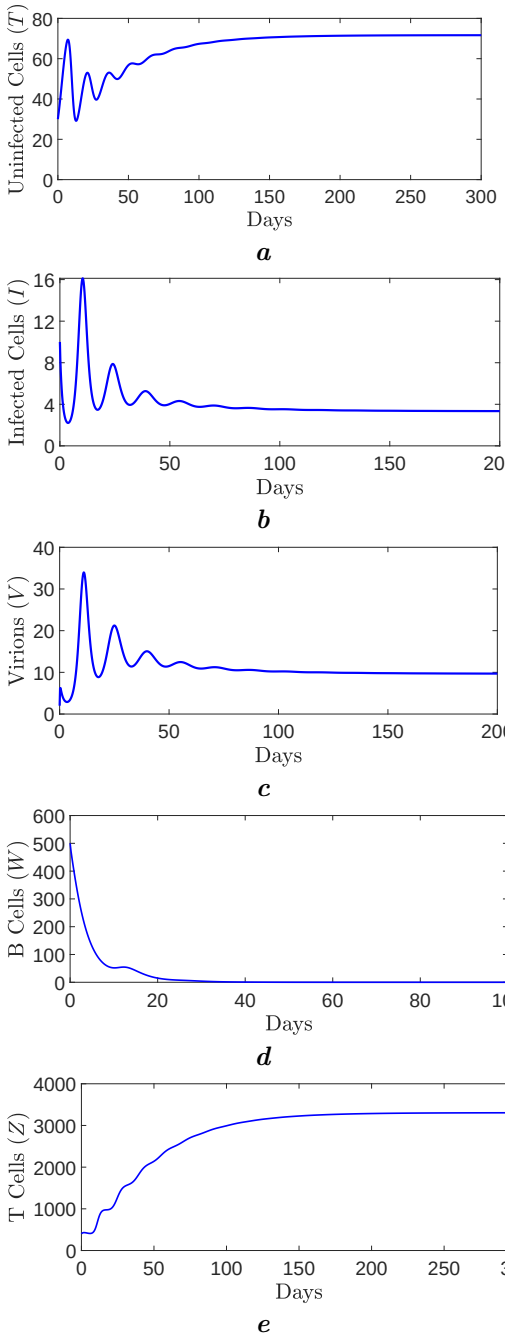

Fig. 5. The infection dynamics illustrating the stability of the third endemic equilibrium E_3.

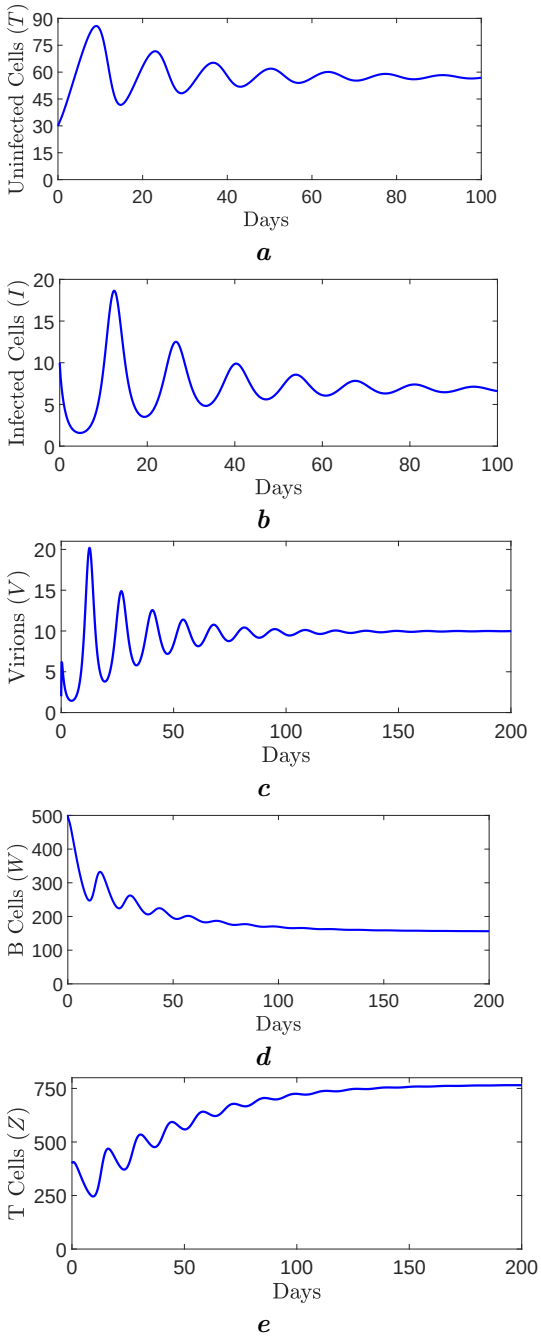

Fig. 6. The infection dynamics illustrating the stability of the fourth endemic equilibrium E_4.

After several days of the infection, we observe from Figure 5 that the humoral immune response is the only component that converges towards zero while the other four problem variables converge towards their respective values of the infected equilibrium $E_3 = (71.7, 3.3, 9.7, 0, 3308.6)$. While, based on Table 3, we have $\mathcal{R}_2 = 2.7673$ and $\mathcal{R}_2^{CTL,W} = 0.0290$, that is to say $\mathcal{R}_2 > 1$ and $\mathcal{R}_2^{CTL,W} < 1$, the simulation supports the theoretical result stated in Theorem 5. Indeed, we can notice that because there exists sufficient amount of infected cells then CTL cells are mobilized to destroy them.

Our last numerical simulations deal with the stability of the last endemic equilibrium. Using Table 3, we get $\mathcal{R}_3 = 1.4104$ and $\mathcal{R}_2^{CTL,W} = 0.0193$. In other terms $\mathcal{R}_3 > 1$ and $\mathcal{R}_2^{CTL,W} < 1$, which demonstrates the stability of E_4 as previously stated in Theorem 6. Indeed, it can be observed from Figure 6 that all the curves converge toward the endemic equilibrium $E_4 = (56.9811, 6.6667, 10, 155.5556, 767.6450)$.

6. Conclusions

In this work, we have presented a mathematical model that describes the dynamics of HCV infection by considering two essential modes of transmission, virus to cell and cell to cell. We have also taken into account the cure of infected cells. The model has included the role of CTL and antibody responses in our suggested hepatitis C virus dynamics. Moreover, we have presented some mathematical analysis, including the existence, positivity, and the boundedness of the unique solution. We have determined the basic reproduction number $\mathcal{R}_0$. Besides, we have found the expressions of reproduction number of the humoral immune, the cellular immune respectively noted by R^W and R^{CTL}. Also, the threshold parameters that describe the average number of secondary generated infected cells in the presence of both humoral and cellular immune are noted respectively by $R_1^{CTL,W}$ and $R_2^{CTL,W}$. Then, the local stability of one disease-free equilibrium and four endemic equilibria are established in terms of the different conditions on the key thresholds $\mathcal{R}_0$, R^W, R^{CTL}, $R_1^{CTL,W}$ and $R_2^{CTL,W}$. The paper ends by some numerical simulations illustrating the behavior of infection by the HCV during the days of observation. Results indicate that the immunity system represented by antibodies and CTL cells reduces the infection under some appropriate conditions. More precisely, we have established that B cells do not stimulate themselves to destroy the virions unless there are sufficient levels of virions. Likewise, T cells do not neutralize the infected cells unless there exist sufficient amounts of infected cells.

[1] https://www.who.int/news-room/fact-sheets/detail/hepatitis-c.

[2] Neumann A. U., Lam N. P., Dahari H., Gretch D. R., Wiley T. E., Layden T. J., Perelson A. S. Hepatitis C Viral Dynamics in Vivo and the Antiviral Efficacy of Interferon-α Therapy. Science. **282** (5386), 103–107 (1998).

[3] Hattaf K., Yousfi N. A Delay Differential Equation Model of HIV with Therapy and Cure Rate. International Journal of Nonlinear Science. **12**, 503–512 (2011).

[4] Hattaf K., Yousfi N., Tridane A. Mathematical analysis of a virus dynamics model with general incidence rate and cure rate. Nonlinear Analysis: Real World Applications. **13** (4), 1866–1872 (2012).

[5] Liu X., Wang H., Hu Z., Ma W. Global stability of an HIV pathogenesis model with cure rate. Nonlinear Analysis: Real World Applications. **12**, 2947–2961 (2011).

[6] Srivastava P. K., Banerjee M., Chandra P. Modeling the drug therapy for HIV infection. Journal of Biological Systems. Journal of Biological Systems. **17** (2), 213–223 (2009).

[7] Tian Y., Liu X. Global dynamics of a virus dynamical model with general incidence rate and cure rate. Nonlinear Analysis: Real World Application. **16**, 17–26 (2014).

[8] Zhou X., Song X., Shi X. A differential equation model of HIV infection of CD4$^+$ $\mathcal{T}$-cells with cure rate. Journal of Mathematical Analysis and Applications. **342** (2), 1342–1355 (2008).

[9] Dahari H., Major M., Zhang X., Mihalik K., Rice M. C., Perelson S. A., Feinstone M. S., Neumann U. A. Mathematical modeling of primary hepatitis C infection: Noncytolytic clearance and early blockage of virion production. Gastroenterology. **128** (4), 1056–1066 (2005).

[10] Reluga T. C., Dahari H., Perelson A. S. Analysis of hepatitis C virus infection models with hepatocyte homeostasis. SIAM Journal on Applied Mathematics. **69** (4), 999–1023 (2009).

[11] Lai X., Zou X. Modeling cell-to-cell spread of HIV-1 with logistic target cell growth. Journal of Mathematical Analysis and Applications. **426** (1), 563–584 (2015).

[12] Mojaver A., Kheiri H. Dynamical analysis of a class of hepatitis C virus infection models with application of optimal control. International Journal of Biomathematics. **9** (3), 3997–4008 (2016).

[13] Pan S., Chakrabarty S. P. Threshold dynamics of HCV model with cell-to-cell transmission and a non-cytolytic cure in the presence of humoral immunity. Communications in Nonlinear Science and Numerical Simulation. **61**, 180–197 (2018).

[14] Avendano R., Esteva L., Flores J. A., Fuentes Allen J. L., Gómez G., López-Estrada Je. A mathematical model for the dynamics of hepatitis C. Journal of Theoretical Medicine. **4**, 109–118 (2002).

[15] Meskaf A., Tabit Y., Allali K. Global analysis of a HCV model with CTL antibody responses and therapy. Applied Mathematical Sciences. **9** (81), 3997–4008 (2015).

[16] Nabi K. N., Podder C. N. Sensitivity analysis of chronic hepatitis C virus infection with immune response and cell proliferation. International Journal of Biomathematics. **13** (3), 301–319 (2020).

[17] Wodarz D. Hepatitis C virus dynamics and pathology: The role of CTL and antibody responses. Journal of General Virology. **84** (7), 1743–1750 (2003).

[18] Wodarz D. Mathematical models of immune effector responses to viral infections: Virus control versus the development of pathology. Journal of Computational and Applied Mathematics. **184** (1), 301–319 (2005).

[19] Yousfi N., Hattaf K., Rachik M. Analysis of a HCV model with CTL and antibody responses. Applied Mathematical Sciences. **3**, 2835–2847 (2009).

[20] Banerjee S., Keval R., Gakkhar S. Modeling the dynamics of hepatitis C virus with combined antiviral drug therapy: Interferon and Ribavirin. Mathematical Biosciences. **245** (2), 235–248 (2013).

[21] Chen S.-S., Cheng C.-Y., Takeuchi Y. Stability analysis in delayed within-host viral dynamics with both viral and cellular infections. Journal of Mathematical Analysis and Applications. **442** (2), 642–672 (2016).

[22] Dahari H., Lo A., Ribeiro R. M., Perelson A. S. Modeling hepatitis C virus dynamics: Liver regeneration and critical drug efficacy. Journal of Theoretical Biology. **247** (2), 371–381 (2007).

[23] Dubey B., Dubey P., Dubey S. U. Modeling the intracellular pathogen-immune interaction with cure rate. Communications in Nonlinear Science and Numerical Simulation. **38**, 72–90 (2016).

[24] Zwillinger D., Jeffrey A. Table of Integrals, Series, and Products. Elsevier (2007).

[25] Hattaf K., Yousfi N. A generalized virus dynamics model with cell-to-cell transmission and cure rate. Advances in Difference Equations. **2016**, 174 (2016).

[26] Li J., Men K., Yang Y., Li D. Dynamical analysis on a chronic hepatitis C virus infection model with immune response. Journal of Theoretical Biology. **365**, 337–346 (2015).

[27] Perasso A. An introduction to the basic reproduction number in mathematical epidemiology. ESAIM: Proceedings and Surveys. **62**, 123–138 (2018).

[28] Reyes-Silveyra J., Mikler A. R. Modeling immune response and its effect on infectious disease outbreak dynamics. Theoretical Biology and Medical Modelling. **13**, 10 (2016).

[29] Van der Driessche P., Watmough J. Reproduction numbers and sub-threshold endemic equilibria for compartmental models of disease transmission. Mathematical Biosciences. **180** (1–2), 29–48 (2002).

[30] Vargas-De-León C. Stability analysis of a model for HBV infection with cure of infected cells and intracellular delay. Applied Mathematics and Computation. **219** (1), 389–398 (2012).

Динамічний аналіз моделі HCV з міжклітинною передачею та швидкістю одужання за наявності адаптивного імунітету

Садкі М.[1], Харруді С.[2], Аллалі К.[1]

[1] *Лабораторія математики, інформатики та застосунків, факультет наук і техніки Мохаммедіа, Університет Хасана II Касабланки, PO Box 146, Мохаммедіа, Марокко*

[2] *Національна школа торгівлі та управління Касабланки, Університет Хасана II, Касабланка, Марокко*

У цій роботі досліджується математично та чисельно динаміку захворювання вірусом гепатиту С з урахуванням двох основних шляхів передачі інфекції, а саме: від вірусу до клітини та від клітини до клітини. У нашій моделі враховується роль швидкості одужання інфікованих клітин та ефект адаптивного імунітету. Модель складається з п'яти нелінійних диференціальних рівнянь, що описують взаємодію між неінфікованими клітинами, інфікованими клітинами, віріонами гепатиту С та адаптивним імунітетом. Цей імунітет подано через гуморальний і клітинний імунні відповіді. Ця робота починається з доведення невід'ємності та обмеженості розв'язків і визначення основного відтворювального числа. Далі встановлено п'ять рівноважних положень, теоретично та чисельно продемонстровано аналіз локальної стійкості для всіх рівноважних положень. Нарешті, доходимо висновку, що чисельні результати узгоджуються з нашими теоретичними положеннями.

Ключові слова: *міжклітинний, швидкість одужання, гуморальна імунна відповідь, клітинна імунна відповідь, адаптивний імунітет, стійкість.*